

Angular dependence of the bulk nucleation field H_{c2} of aligned MgB_2 crystallites

O. F. de Lima, C. A. Cardoso, R. A. Ribeiro, M. A. Avila, and A. A. Coelho
*Instituto de Física "Gleb Wataghin", UNICAMP, 13083-970, Campinas-SP,
Brazil*

Abstract

The angular dependence of the bulk nucleation field of a sample made of aligned MgB_2 crystallites was obtained using dc magnetization and ac susceptibility measurements. A good fitting of the data by the three-dimensional anisotropic Ginzburg-Landau theory attests the bulk nature of the critical field H_{c2} . We found a mass anisotropy ratio $\varepsilon^2 \approx 0.39$ that implies an anisotropy of the Fermi velocity, with a ratio of 1.6 between the in-plane and perpendicular directions, if an isotropic gap energy is assumed. For an s-wave anisotropic gap this ratio could increase to 2.5. Besides the fundamental implications of this result, it also implies the use of texturization techniques to optimize the critical current in wires and other polycrystalline forms of MgB_2 .

74.25.Ha, 74.60.Ec, 74.60.Ge, 74.70.Ad

Recent studies on the new MgB₂ superconductor¹, with a critical temperature $T_c = 39$ K, have evidenced its potential for applications^{2,3}, although intense magnetic relaxation effects limit the critical current density, J_c , at high magnetic fields⁴. This means that effective pinning centers must be added⁵ into the material microstructure, in order to halt dissipative flux movements. Concerning the basic microscopic mechanism to explain the superconductivity in MgB₂, several experimental^{6–12} and theoretical^{13–15} works have pointed to the relevance of a phonon-mediated interaction, in the framework of the BCS theory. Questions have been raised about the relevant phonon modes, and the gap and Fermi surface anisotropies, in an effort to interpret spectroscopic and thermal data that give values between 2.4 and 4.5 for the ratio $2\Delta_0/kT_c$, where Δ_0 is the gap energy and k is the Boltzmann constant. Preliminary results on the H_{c2} anisotropy have shown values of the ratio between the in-plane and perpendicular directions which are around 1.7 for aligned MgB₂ crystallites¹⁶, 1.8 for *c*-axis oriented thin films¹⁷, 2.6 for small single crystals^{18,19}, and 1.3 for very clean epitaxial thin films²⁰. Specific heat¹⁰ and electron spin resonance²¹ studies have also shown broadening effects consistent with an H_{c2} anisotropy. Here we present a study on the angular dependence of H_{c2} that points to a Fermi velocity anisotropy around 2.5. Besides the fundamental aspects of this new result, it also points clearly to the necessity of using texturization techniques to optimize J_c in wires and other polycrystalline components of MgB₂.

We measured a sample of well-aligned MgB₂ crystallites whose preparation details have been described elsewhere¹⁶. Briefly, a MgB₂ powder of almost 100% crystallites, having sizes up to $30 \times 20 \times 5 \mu\text{m}^3$, was obtained from a weakly sintered material reacted at a temperature $T = 1200 \text{ }^\circ\text{C}$, much higher than the currently reported values below $900 \text{ }^\circ\text{C}$. By spreading this powder on both sides of a paper we aligned the crystallites with their *ab* planes sitting on the paper surface. Several samples were then mounted consisting of a pile of five squares of $3 \times 3 \text{ mm}^2$, cut from the *crystallite-painted* paper and glued with Araldite resin.

Measurements of the magnetic moment and ac susceptibility were performed, respec-

tively, with a SQUID magnetometer (model MPMS-5) and a PPMS-9T machine, both made by Quantum Design. In order to obtain the angular dependence under an axial applied field a sample holder was built as sketched in Fig. 1. All parts were machined from a teflon rod, except the removable acrylic protractor, which is about 40 times larger than the hollow box. The MgB₂ sample (in black) is mounted vertically inside the box that is tightly inserted into a 5 mm diameter hole. This hole is drilled in the plane surface of the sectioned rod that, finally, is attached at the end of the system transport stick. A squared opening was made in the protractor's center such that it fits precisely around the box sides. In this way we are able to rotate the sample with a precision of ± 0.5 deg, which is good enough in view of the crystallites misalignment, evaluated¹⁶ to be 2.3 deg around the sample *c* axis. The inconvenience of taking the sample holder out of the system, every time that a new angle has to be set, is compensated by its simplicity and small magnetic background.

Fig. 2 shows the magnetic field dependence of the magnetization in $T = 25$ K, for a few representative angles, θ , between the sample *c* axis and the magnetic field direction. The inset displays a relatively sharp transition with onset at $T_c = 39$ K, measured with $H = 10$ Oe in a zero-field cooling (ZFC) and field-cooling measured on cooling (FCC) procedures. The ZFC measurements shown in the main frame look noisy possibly due to the effect of intense vortex creep⁴, combined with a complex regime of flux penetration in the granular sample. The occurrence of random weak links and the varied coupling between grains produce a fluctuating behavior in the sample overall response. However, in all cases we were able to define $H_{c2}(\theta)$, at the crossing point between the horizontal baseline and the straight line drawn across the experimental points in the region near the onset of transition. This linear behavior of the magnetization close to the onset is indeed expected from the Ginzburg-Landau (G-L) theory²². A constant paramagnetic background was subtracted from all sets of data. In fact, one of the reasons for measuring at 25 K is because at this temperature $H_{c2}(\theta)$ ranges between 28 - 36 kOe, where the paramagnetic background is saturated¹⁶. Fig. 3 is a plot of ZFC followed by FCC magnetization measurements (for $\theta = 85$ deg and $T = 25$ K) displaying clearly an irreversibility field $H_{irr} \simeq 0.88 H_{c2}$. This

amount of separation between H_{irr} and H_{c2} is similar to those observed in c-axis oriented thin films¹⁷, and contrasts with $H_{irr} \simeq 0.5 H_{c2}$ observed for untextured bulk samples^{2,5,23}. Another significant difference is that the slope dH_{c2}/dT , close to T_c , is around 0.44 T/K for untextured bulk samples²³, while it is between 0.2 ~ 0.3 T/K for textured samples¹⁶ and single crystals¹⁹. We believe that, besides the fact that MgB₂ untextured samples give only an average response of its anisotropic properties, the samples degree of purity might play also an important role, since it affects the electronic mean free path.

Fig. 4 displays $H_{c2}(\theta)$ for θ between - 20 deg and 120 deg. The vertical error bars were estimated to be around ± 1 kOe while the horizontal error bars, of ± 2.5 deg, almost coincide with the symbol size. The solid line going through the experimental points represents a good fit of the angular dependence, predicted by the 3D anisotropic G-L theory to be^{22,24} $H_{c2}(\theta) = H_{c2}^c [\cos^2(\theta) + \varepsilon^2 \sin^2(\theta)]^{-0.5}$, where $\varepsilon^2 = m_{ab}/m_c = (H_{c2}^c/H_{c2}^{ab})^2$ is the mass anisotropy ratio and H_{c2}^c/H_{c2}^{ab} is the ratio between the bulk nucleation field along the c direction and parallel to the ab planes. We found $\varepsilon^2 \approx 0.39 \pm 0.01$, giving $H_{c2}^c/H_{c2}^{ab} \approx 0.62$, which is close to the value of 0.59 anticipated¹⁶ by ac susceptibility measurements done for the two extreme θ positions, at 0 and 90 degrees. Fig. 4 shows also five data points ($\theta = 0, 25, 65, 85, 90$ deg) marked with stars, which were obtained at the onset of transition of the real part of the complex susceptibility, measured with an excitation field of amplitude 1 Oe and frequency 5 kHz. From $H_{c2}^{ab}/H_{c2}^c = \xi_{ab}/\xi_c \approx 1.6$, $H_{c2}^c(T) = \Phi_0/(2\pi\xi_{ab}^2)$, and using the G-L mean field expression²² for the coherence length $\xi(T) = \xi_0(1 - T/T_c)^{-0.5}$, we find $\xi_{0ab} \approx 65$ Å and $\xi_{0c} \approx 40$ Å, the coherence length at $T = 0$ in the ab planes and along the c axis, respectively. The quantum of flux, in CGS units, is $\Phi_0 = 2.07 \times 10^{-7}$ G cm². The ratio $H_{c2}^{ab}/H_{c2}^c \approx 1.6$ reminds the relationship predicted for the surface nucleation field²⁵ $H_{c3} \approx 1.7 H_{c2}$. However, this is clearly not the case of our data, as one can see from the expected angular dependence of $H_{c3}(\theta)$ for thick samples²⁶, which is plotted in Fig. 4 as a dash-dotted curve. The dashed curve in between represents the well-known Tinkham's formula²⁷ for the surface nucleation field in very thin films. Therefore, a characteristic feature of the surface nucleation field is the cusplike curve shape near $\theta = 90$ deg, which contrasts with the sinusoidal shape followed

by our data.

The macroscopic H_{c2} anisotropy can be caused by an anisotropic gap energy or by an anisotropic Fermi surface, as well as by a combination of both effects²⁸. Assuming an isotropic gap, one gets $\xi_{ab}/\xi_c = V_F^{ab}/V_F^c$, since²² $\xi \propto V_F/\Delta_0$. Therefore, our data implies $V_F^{ab} \approx 1.6 V_F^c$, for the Fermi velocities within the ab plane and along the c direction. However, several experimental^{8,10,11} and theoretical¹³⁻¹⁵ works have suggested an anisotropic gap energy for MgB₂. In particular, two recent reports^{11,15} rely on the analysis of spectroscopic and thermodynamic data to propose an anisotropic s-wave pairing symmetry, such that a minimum gap value, $\Delta_0 \approx 1.2 kT_c$, occurs within the ab plane. Using this result and assuming an isotropic Fermi surface the expected H_{c2} anisotropy would be¹⁵ $H_{c2}^{ab}/H_{c2}^c \approx 0.8$. This conflicts with our present findings and with other results^{16,17} that show clearly $H_{c2}^{ab} > H_{c2}^c$. However, by allowing a Fermi surface anisotropy in their model, Haas and Maki have found that²⁹ $V_F^{ab} \approx 2.5 V_F^c$ in order to match our result of $H_{c2}^{ab}/H_{c2}^c \approx 1.6$, at $T = 25$ K. Therefore the two fundamental sources of microscopic anisotropy affect the H_{c2} anisotropy of MgB₂ in opposite ways. As a consequence of combining both effects to explain the H_{c2} anisotropy, the Fermi velocity anisotropy becomes about 60% higher when compared with the isotropic gap hypothesis. Interestingly, a calculation based on a two-band model has also found³⁰ $V_F^{ab} \approx 2.5 V_F^c$, while a smaller value of $V_F^{ab} \approx 1.03 V_F^c$ was found in a band structure calculation using a general potential method¹³.

The relatively large scattering of reported values for the anisotropy ratio¹⁶⁻²⁰ H_{c2}^{ab}/H_{c2}^c , varying between $1.3 \sim 2.6$, could possibly be ascribed to at least three factors. The first is the sample purity, since it affects directly the energy gap anisotropy at the microscopic level^{24,28}. The second is the experimental criterion used to define H_{c2} , since a reliable bulk transition should be guaranteed. The third factor is that a possible temperature dependent anisotropy ratio could arise from a temperature dependent gap anisotropy^{15,29}. Therefore, results obtained with samples of different purity levels and measured at different temperatures most possibly should not produce the same anisotropy ratios. This is clearly an area deserving much research work.

Concluding, the H_{c2} anisotropy ratio for MgB₂ implies an anisotropy ratio of the Fermi velocity of at least $V_F^{ab}/V_F^c \approx 1.6$, for an isotropic gap energy hypothesis. In a more realistic scenario, of an s-wave anisotropic gap, this ratio could increase to $V_F^{ab}/V_F^c \approx 2.5$. Finally, since J_c is proportional to ξ^2 , it is worth noticing that³¹ $J_c(H // c) / J_c(H // ab) \approx \xi_{ab}/\xi_c \approx H_{c2}^{ab}/H_{c2}^c$. Therefore, we anticipate that the in-plane critical current density values are expected to be about 60% higher than the values along the c direction ($H // ab$). Indeed this J_c anisotropy could be even higher, as suggested by the larger H_{c2} anisotropy observed in thin films¹⁷ and single crystals^{18,19}. This means that, in order to optimize J_c in MgB₂ wires or other polycrystalline components, some texturization technique will be required.

We thank S. Haas, A. V. Narlikar and O. P. Ferreira for useful discussions and acknowledge the financial support from the Brazilian Science Agencies FAPESP and CNPq.

FIGURE CAPTIONS

Figure 1 - Sketch of the sample holder used to get the angular dependence of the sample magnetization in a SQUID magnetometer. The sample (in black) is inside the hollow box, that is tightly inserted into a 5 mm diameter hole. The removable acrylic protractor fits precisely around the box in order to indicate the angular position.

Figure 2 - Zero Field Cooling magnetization measurements as a function of the applied field, for $\theta = 0, 65, 80, 90$ degrees. The bulk nucleation field $H_{c2}(\theta)$ is defined at the crossing of the auxiliary straight lines and the horizontal baseline ($M = 0$). The inset shows ZFC and FCC magnetization measurements as a function of temperature for $H = 10$ Oe, giving $T_c \approx 39$ K.

Figure 3 - Zero Field Cooling (ZFC) followed by Field Cooling on Cooling (FCC) magnetization measurements, for $\theta = 85$ deg and $T = 25$ K. The irreversibility field H_{irr} and upper critical field H_{c2} are indicated by vertical arrows.

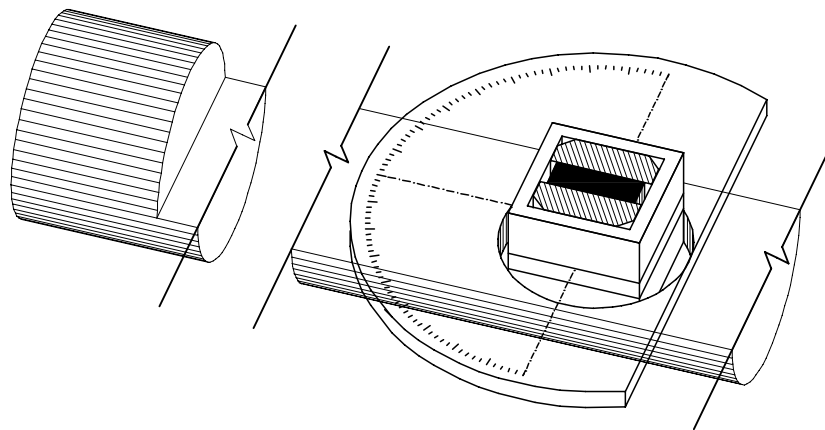
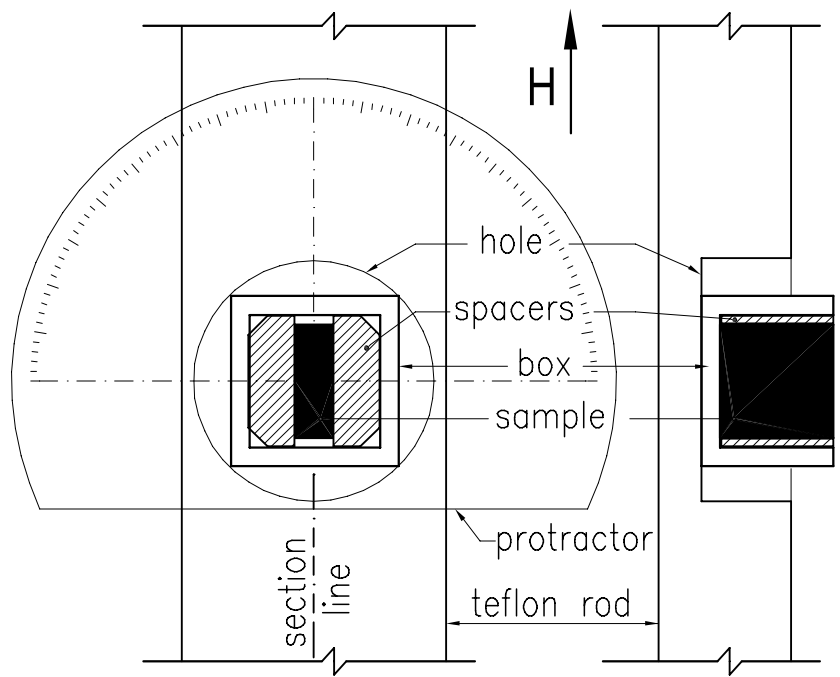
Figure 4 - Bulk nucleation field (or upper critical field), H_{c2} , as a function of the angle, θ , between the sample c axis and the magnetic field direction. Plots of the expected angular dependence for the surface nucleation field, H_{c3} , in thick samples (dash-dotted curve) and very thin films (dashed curve) are also shown. The stars at $\theta = 0, 25, 65, 85, 90$ degrees represent $H_{c2}(\theta)$ obtained at the onset of transition of the real part of ac susceptibility measurements.

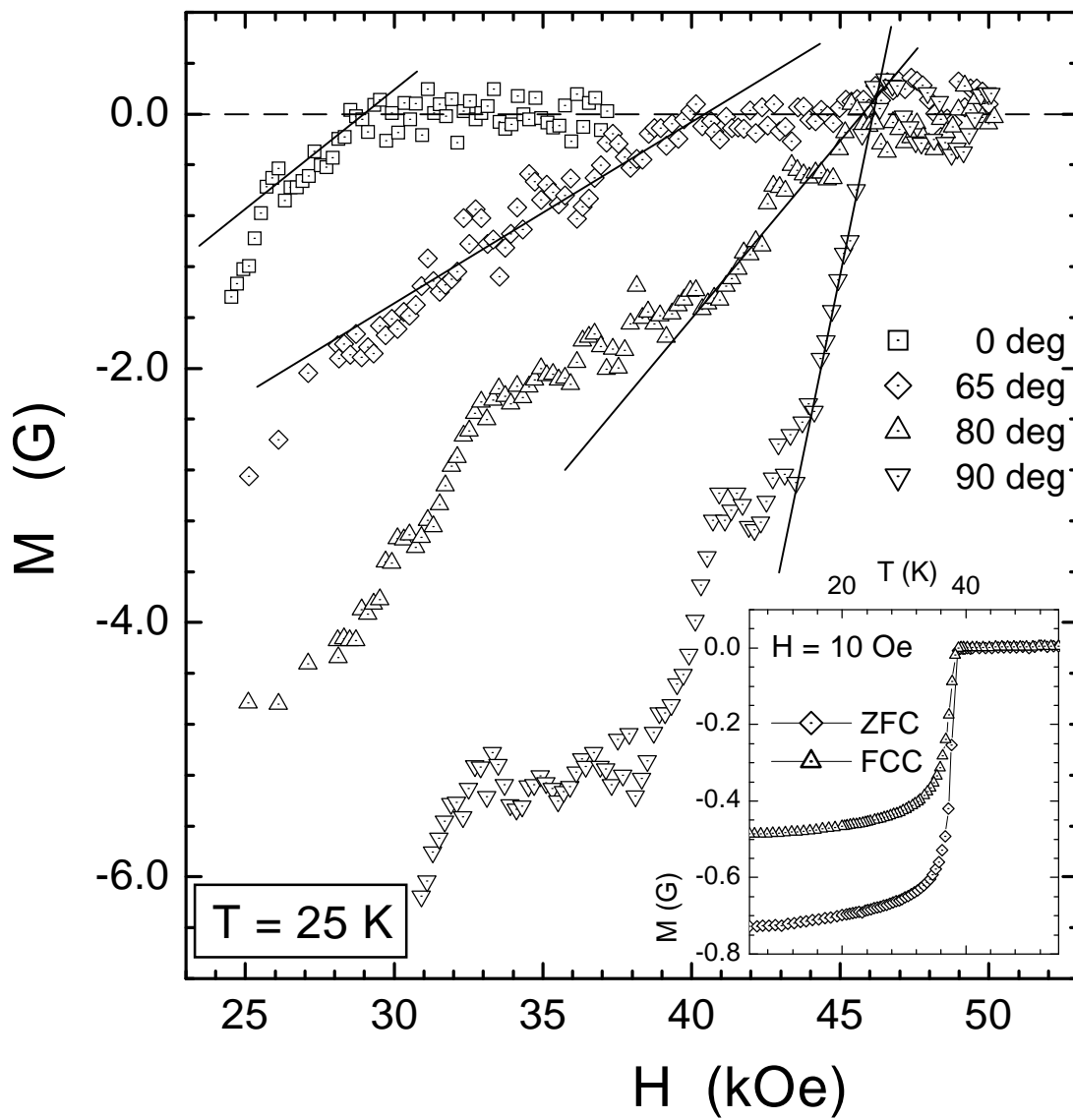
REFERENCES

- ¹ J. Nagamatsu, N. Nakagawa, T. Muranaka, Y. Zenitani, and J. Akimitsu, *Nature* **410**, 63 (2001).
- ² D. C. Larbalestier, L. D. Coonley, M. Rikel, A. A. Polyanskii, J. Jiang, S. Patnaik, X. Y. Cai, D. M. Feldmann, A. Gurevich, A. A. Squitieri, M. T. Naus, C. B. Eom, E. E. Hellstrom, R. J. Cava, K. A. Regan, N. Rogado, A. Hayward, T. He, J. S. Slusky, P. Khalifah, I. Inumaru, and M. Haas, *Nature* **410**, 186 (2001).
- ³ P. C. Canfield, D. K. Finnemore, S. L. Bud'ko, J. E. Ostenson, G. Lapertot, C. E. Cunningham, and C. Petrovic, *Phys. Rev. Lett.* **86**, 2423 (2001).
- ⁴ Y. Bugoslavsky, G. K. Perkins, X. Qi, L. F. Cohen, and A. D. Caplin, *Nature* **410**, 563 (2001).
- ⁵ Y. Bugoslavsky, L. F. Cohen, G. K. Perkins, M. Polichetti, T. J. Tate, R. Gwilliam, and A. D. Caplin, *Nature* **411**, 561 (2001).
- ⁶ S. L. Bud'ko, G. Lapertot, C. Petrovic, C. E. Cunningham, N. Anderson, and P. C. Canfield, *Phys. Rev. Lett.* **86**, 1877 (2001).
- ⁷ G. Karapetrov, M. Iavarone, W. K. Kwok, G. W. Crabtree, and D. G. Hinks, *Phys. Rev. Lett.* **86**, 4374 (2001).
- ⁸ Y. Wang, T. Plackowski and A. Junod, *Physica C* **355**, 179 (2001).
- ⁹ T. Yildirim, O. Gülseren, J. W. Lynn, C. M. Brown, T. J. Udovic, Q. Huang, N. Rogado, K. A. Regan, M. A. Hayward, J. S. Slusky, T. He, M. K. Haas, P. Khalifah, K. Inumaru, and R. J. Cava, *Phys. Rev. Lett.* **87**, 037001 (2001).
- ¹⁰ F. Bouquet, R. A. Fisher, N. E. Philips, D. G. Hinks, and J. D. Jorgensen, *Phys. Rev. Lett.* **87**, 047001 (2001).
- ¹¹ C.-T. Chen, P. Seneor, N.-C. Yeh, R. P. Vasquez, C. U. Jung, Min-Seok Park, Heon-Jung

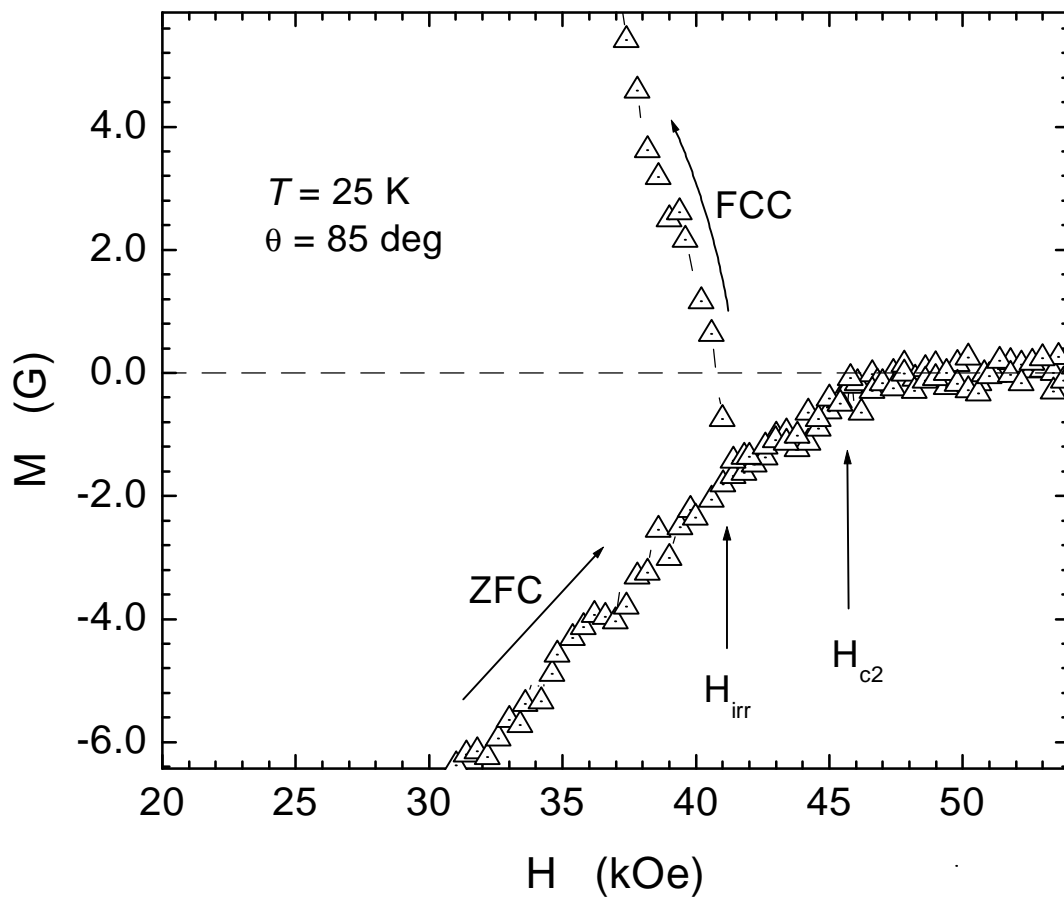
- Kim, W. N. Kang, and Sung-Ik Lee, Preprint cond-mat/0104285 (2001).
- ¹² H. Martinho, A. A. Martin, C. Rettori, O. F. de Lima, R. A. Ribeiro, M. A. Avila, P. G. Pagliuso, N. O. Moreno, and J. L. Sarrao, Preprint cond-mat/0105204 v2 (2001).
- ¹³ J. Kortus, I. I. Mazin, K. D. Belashchenko, V. P. Antropov and L. L. Boyer, Phys. Rev. Lett. **86**, 4656 (2001).
- ¹⁴ J. M. An and W. E. Pickett, Phys. Rev. Lett. **86**, 4366 (2001).
- ¹⁵ S. Haas and K. Maki, Preprint cond-mat/0104207 (2001).
- ¹⁶ O. F. de Lima, R. A. Ribeiro, M. A. Avila, C. A. Cardoso, and A. A. Coelho, Phys. Rev. Lett. **86**, 5974 (2001).
- ¹⁷ S. Patnaik, L. D. Cooley, A. Gurevich, A. A. Polyanskii, J. Jiang, X. Y. Cai, A. A. Squitieri, M. T. Naus, M. K. Lee, J. H. Choi, L. Belenky, S. D. Bu, J. Letteri, X. Song, D. G. Schlom, S. E. Babcock, C. B. Eom, E. E. Hellstrom, and D. C. Larbalestier, Supercond. Sci. Technol. **14**, 315 (2001).
- ¹⁸ S. Lee, H. Mori, T. Masui, Yu. Eltsev, A. Yamamoto, and S. Tajima, Preprint cond-mat/0105545 (2001).
- ¹⁹ M. Xu, H. Kitazawa, Y. Takano, J. Ye, K. Nishida, H. Abe, A. Matsushita, and G. Kido, Preprint cond-mat/0105271 (2001).
- ²⁰ M. H. Jung, M. Jaime, A. H. Lacerda, G. S. Boebinger, W. N. Kang, H. J. Kim, E. M. Choi, and S. I. Lee, Preprint cond-mat/0106146 (2001).
- ²¹ F. Simon, A. Jánossy, T. Fehér, F. Murányi, S. Garaj, L. Forró, C. Petrovic, S. L. Bud'ko, G. Lapertot, V. G. Kogan, and P. C. Canfield, Phys. Rev. Lett. **87**, 047002 (2001).
- ²² M. Tinkham, *Introduction to Superconductivity*, 2nd ed. (McGraw-Hill, New York, 1996).
- ²³ D. K. Finnemore, J. E. Ostenson, S. L. Bud'ko, G. Lapertot, and P. C. Canfield, Phys.

- Rev. Lett. **86**, 2420 (2001).
- ²⁴ D. R. Tilley, Proc. Phys. Soc. London **86**, 289 (1965).
- ²⁵ D. Saint-James and P. G. de Gennes, Physics Letters **7**, 306 (1963).
- ²⁶ K. Yamafuji, E. Kusayanagi and F. Irie, Physics Letters **21**, 11 (1966).
- ²⁷ M. Tinkham, Physics Letters **9**, 217 (1964).
- ²⁸ H. W. Weber (editor), *Anisotropy Effects in Superconductors* (Plenum Press, New York, 1977).
- ²⁹ S. Haas, private communications.
- ³⁰ S. V. Shulga, S. -L. Drechsler, H. Eschrig, H. Rosner, and W. E. Pickett, Preprint cond-mat/0103154 (2001).
- ³¹ G. Blatter, M. V. Feigel'man, V. B. Geshkenbein, A. I. Larkin, and V. M. Vinokur, Rev. Mod. Phys. **66**, 1125 (1994).

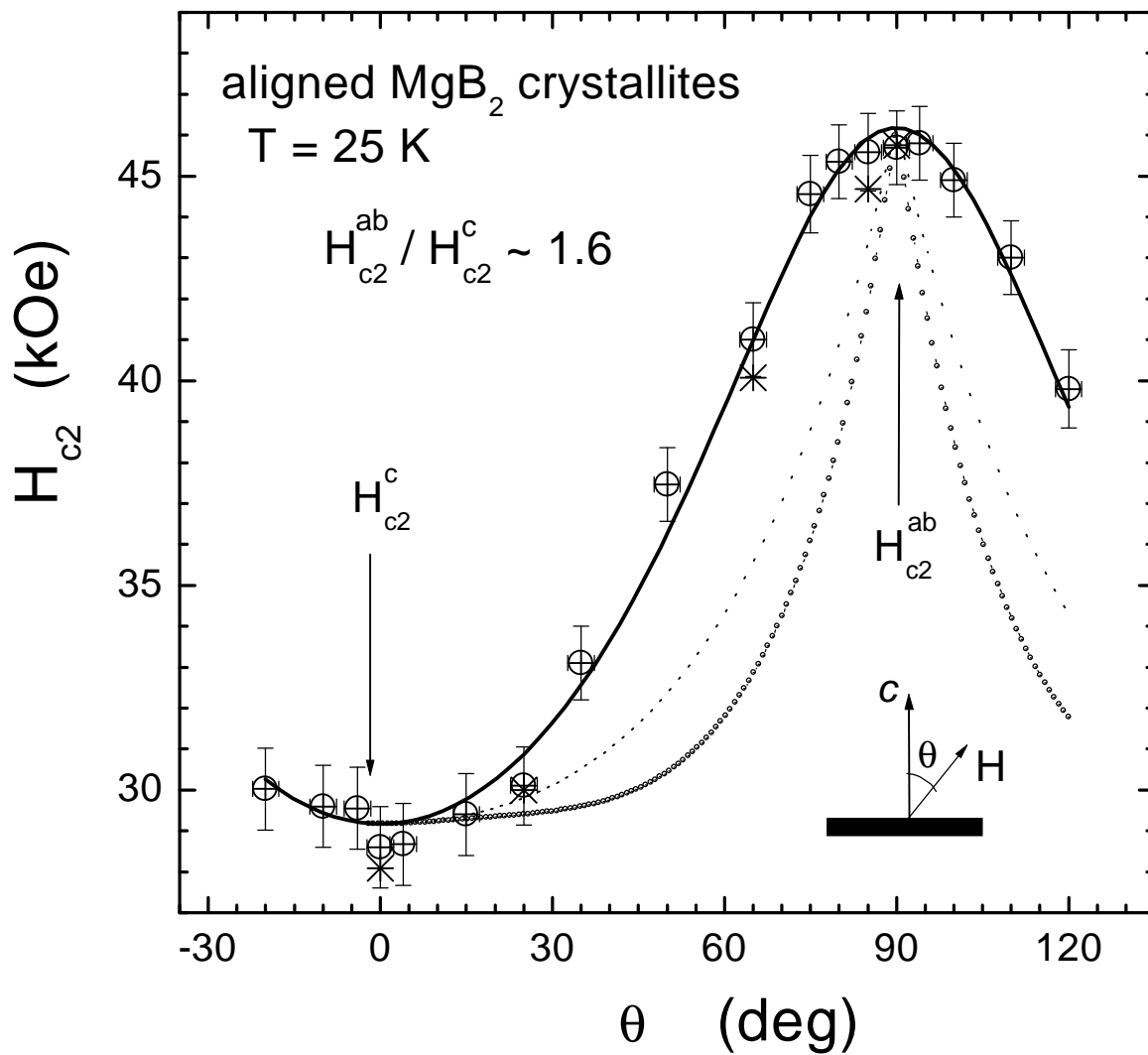




de Lima et al. - Fig. 2



de Lima et al. - Fig. 3



de Lima et al. - Fig. 4